

# A Thin Film Phantom for Blood Flow Simulation and Doppler Test

Stephen McAleavey, Zaegyoo Hah, and Kevin Parker, *Fellow, IEEE*

**Abstract**—The thin film phantom is a new type of ultrasound resolution test object. It consists of a thin planar substrate that is acoustically matched to the surrounding media. Precisely located scatterers on the surface of the substrate generate echo signals. The patterning of scatterers on the substrate allows echogenicity to be controlled as a function of position, which enables the production of a test object with highly reproducible and controllable scattering characteristics.

We show that by vibrating the substrate in a suitable manner, an echo signal may be generated that simulates bi-directional flow. We demonstrate that a vibration of low amplitude at frequency  $f_0$  produces a Doppler spectral signal at  $f_0$  and  $-f_0$ , within the limits of aliasing. Furthermore, by driving the film with a bandlimited noise signal, we illustrate how a velocity distribution may be simulated. A time-varying flow velocity may be simulated by varying the noise bandwidth with time. Finally, using this technique, we demonstrate a system that simulates an arterial flow pattern, including its characteristic velocity distribution in forward and reverse directions simultaneously.

## I. INTRODUCTION

PHYSIOLOGICAL blood flow always involves some degree of velocity gradient because of the viscosity of blood [1]. Furthermore, the flow profile can vary significantly, even within the same vessel, over time. To test the performance of Doppler systems in the presence of flow gradients, it is useful to have a phantom that can produce echo signals that mimic those produced by flowing blood. Simulation of these flow gradients with a conventional flow phantom is not a simple task.

Flow phantoms using blood-mimicking fluids and pumps have been constructed that capture many of the features of flow in tissue, including velocity gradients and, in some cases, time-varying flow [2]–[5]. Hoskins *et al.* [2] demonstrated a system wherein a computer-controlled pump generates a time-varying flow through a tissue-mimicking phantom. The flow generated is similar to actual arterial flow, including a reverse flow component. A phantom demonstrated by Boote and Zagzebski [5] also produces a pulsatile flow. Such phantoms represent the “gold-standard” for flow simulation but are complex in their design, operation, and maintenance.

Manuscript received April 13, 2000; accepted November 14, 2000. The authors are grateful for support from the NIH SBIR grant program (1 R43 HL62041-01A1).

The authors are with the Department of Electrical and Computer Engineering, University of Rochester, Rochester, NY 14627 (e-mail: mcaleave@ece.rochester.edu).

Moving string and belt phantoms are simpler from a mechanical standpoint than flow phantoms [6]–[8]. Time-varying flow is simulated with some of these devices by changing the velocity of the string or belt in time, as in the work of Russell *et al.* [6]. Rickey and Fenster [7] have presented a moving belt phantom, where a stationary clutter signal is superimposed on the moving belt echo. String and belt phantoms are simpler to operate than flow phantoms but have a limited ability to simulate velocity gradients.

Here we present a phantom capable of simulating time-varying and velocity-dispersed flow. The peak flow velocity, the flow profile, and the flow rate versus time are all controllable. This is achieved with a solid, thin film as a test target, using a simple piezoelectric element to induce small-scale motion of the film. A consequence of this approach, however, is that the simulated flow appears to be bi-directional. That is, simulation of flow toward the transducer at velocity  $v$  also results in simulated flow away from the transducer at the same velocity. At least one commercial phantom (DSP-1; JJA Instruments) uses a vibrating target to generate a Doppler signal. The phantom described here, however, allows a greater degree of control over the Doppler signal than any other vibrating target phantoms of which the authors are aware.

## II. THEORY

Holen *et al.* [9] demonstrated that a vibrating target results in a frequency modulation of the toneburst used in Doppler ultrasound. They showed that sinusoidally oscillating structures can produce Doppler signals in which energy is focused at integer multiples of the vibration frequency, when the vibration cycle is shorter than the FFT (fast Fourier transform) window size. The energy weighting of each frequency multiple is determined by a Bessel function of the first kind [10].

### A. Echo Signal

An expression for the echo received from an oscillating point target may be developed with the aid of a range-time graph (Fig. 1), as in [1] and [11]. The graph depicts the relationship of the target, the transducer, and the sound pulse; the range dimension along the abscissa; and the temporal dimension along the ordinate. The target, located a mean distance  $d_0$  from the transducer, is immersed in a propagating medium with speed of sound  $c$ . The position of the scatterer is given by  $x(t) = d_0 + A \cos(\omega_0 t)$ , where

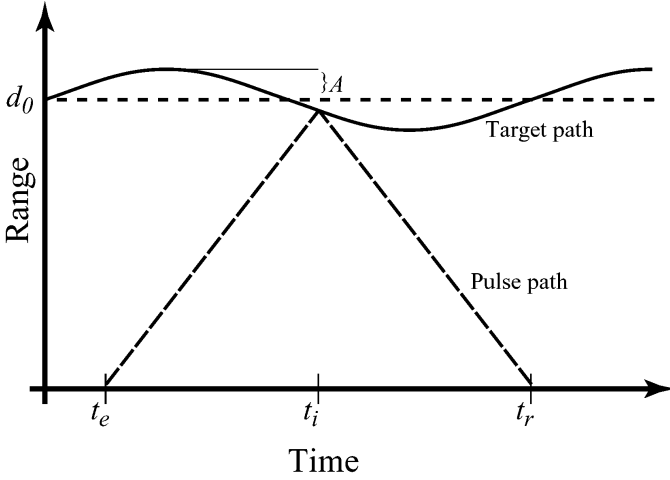


Fig. 1. Range-time graph depicting the relationship between target and pulse position in time.

$A$  is the vibration amplitude and  $\omega_0$  is the vibration frequency. The transducer, located at  $x = 0$ , launches a pulse at time  $t_e$  toward the target. If we let  $t_i$  be the time when the pulse and target interact, then

$$(t_i - t_e)c = d_0 + A \cos(\omega_0 t_i) \quad (1)$$

To aid in calculating  $t_i$ , we break it into three parts, letting  $t_i = t_e + d_0/c + \varepsilon$ , where the  $d_0/c$  term represents the average path delay between the source and target and  $\varepsilon$  is the component of the delay caused by the target oscillation. Eq. (1) may then be rewritten as

$$t_i - t_e = \frac{d_0}{c} + \frac{A}{c} \cos \left( \omega_0 \left( \frac{d_0}{c} + \varepsilon + t_e \right) \right). \quad (2)$$

Eq. (2) may be expanded in a Taylor series on  $\varepsilon$

$$t_i - t_e \approx \frac{d_0}{c} + \frac{A}{c} \left\{ \cos \left( \omega_0 \left[ \frac{d_0}{c} + t_e \right] \right) - \omega_0 \varepsilon \sin \left( \omega_0 \left[ \frac{d_0}{c} + t_e \right] \right) - \dots \right\}.$$

The maximum value of  $\varepsilon$  is  $A/c$ . For typical values of the parameters ( $A \approx 10^{-4}$  m,  $c \approx 1500$  m/s,  $\omega_0 \approx 10^3$ ),  $\omega_0 \varepsilon$  is on the order of  $10^{-4}$ . Thus, we may calculate  $t_i$  by evaluating  $x(t)/c$  at  $t = d_0/c + t_e$  without incurring significant error, and

$$t_i = \frac{d_0}{c} + \frac{A}{c} \cos \left\{ \omega_0 \left( \frac{d_0}{c} + t_e \right) \right\} + t_e.$$

Let us define a propagation time  $t_p$  as  $t_p = t_i - t_e$ . The return path for the pulse is identical to the transmit path; thus, the time of reception of the pulse  $t_r$  is  $t_e + 2t_p$  and

$$t_r = \frac{2d_0}{c} + \frac{2A}{c} \cos \left\{ \omega_0 \left( \frac{d_0}{c} + t_e \right) \right\} - t_e.$$

Solving for  $t_e$ ,

$$t_e \approx t_r - \frac{2d_0}{c} - \frac{2A}{c} \cos \left\{ \omega_0 \left( t_r - \frac{d_0}{c} \right) \right\}$$

where the approximation is due to neglect of a  $2\omega_0 \varepsilon$  term in the argument of the cosine. For typical values of  $\omega_0$  ( $\sim 10^3$ ) and  $\varepsilon$  ( $\sim 10^{-6}$ ), this yields a negligible error.

Let us call the transmitted signal  $s(t)$ . Assuming a linear propagation model, the received signal from a point target will be a delayed and scaled version of the transmitted signal. Using the relationship  $t_r - t_e = 2t_p$  and replacing  $t_r$  with  $t$ , we obtain

$$r(t) = \alpha s \left( t - \frac{2d_0}{c} - \frac{2A}{c} \cos \left\{ \omega_0 \left( t - \frac{d_0}{c} \right) \right\} \right). \quad (3)$$

Given this expression for the received signal in terms of the transmitted signal, we are now in a position to estimate the response of continuous wave (CW) and pulsed wave (PW) Doppler systems to a vibrating target.

### B. CW Doppler Signal

For CW systems, the transmitted ultrasound signal is  $s(t) = \cos(\omega_c t)$ , where  $\omega_c$  is the radian frequency of the signal. Substituting this expression for  $s(t)$  into (3) yields

$$r(t) = \alpha \cos \left( \omega_c \left\{ t - \frac{2d_0}{c} - \frac{2A}{c} \cos \left( \omega_0 \left\{ t - \frac{d_0}{c} \right\} \right) \right\} \right).$$

Typical Doppler systems perform quadrature demodulation, where the received signal is multiplied with in-phase and quadrature sinusoids at the transmit frequency and low-pass filtered, as described in [1]. Because the amplitude of target oscillation is small, the demodulated signal may be approximated as

$$r_d(t) \approx \frac{1}{2} e^{j \left( \frac{2d_0 \omega_c}{c} \right)} \left\{ 1 + j \frac{2A \omega_c}{c} \cos \left( \omega_0 \left\{ t - \frac{d_0}{c} \right\} \right) \right\}. \quad (4)$$

From (4), we see that the demodulated signal is identical to the target vibration signal to within a phase shift and scaling. Thus, the output frequency of the CW Doppler instrument will be equal to the target oscillation frequency as long as the small angle approximation is satisfied.

### C. PW Doppler Signal

For PW Doppler systems, the transmitted signal is a train of windowed sinusoid bursts,

$$s(t) = \sum_n \pi \left( \frac{1}{T} \left\{ t - \frac{2\pi n k}{\omega_c} \right\} \right) \cos \left( \omega_c \left\{ t - \frac{2\pi n k}{\omega_c} \right\} \right),$$

where  $k$  is an integer, and  $\omega_c/k$  is the pulse repetition frequency (PRF).  $\Pi$  is a rectangular window function, equal

to 1 from  $-0.5$  to  $0.5$  and 0 elsewhere.  $T$  is the window length. Substitution into (3) yields

$$r(t) = \sum_n \pi \left( \frac{1}{T} \varphi_n(t) \right) \cos \left( \omega_c \varphi_n(t) \right)$$

where

$$\varphi_n(t) = t - \frac{2\pi nk}{\omega_c} - \frac{2d_0}{c} - \frac{2A}{c} \cos \left( \omega_0 \left\{ t - \frac{2d_0}{c} \right\} \right).$$

A baseband signal is obtained by multiplication with a synchronized complex sinusoid, low-pass filtering, and sampling [1]. The demodulated signal is given by

$$r_{d,n} = 1 + j \frac{2A\omega_c}{c} \cos \left\{ \omega_0 \left( \frac{2\pi nk}{\omega_c} + \frac{d_0}{c} \right) \right\} \quad (5)$$

under the small angle approximations. Here, as in the CW case, the demodulated signal is a scaled, phase-shifted version of the vibration signal. In the PW case, the signal is sampled at the PRF  $\omega_c/k$ .

#### D. General Vibration Signals

From (4) and (5), it is seen that both CW and PW Doppler presented with a vibrating target generate output signals whose frequency is identical to that of the target vibration signal. Furthermore, as long as the restrictions on the amplitude of vibration are observed, that is, that  $2A\omega_c/c \ll 1$ , the process is approximately linear. Thus, not only simple sinusoids but any low amplitude signal may be applied to the target to generate a particular Doppler signal. For a vibration signal  $\nu(t)$ , the output of the PW Doppler system would be

$$r_{d,n} = 1 + j \frac{2A\omega_c}{c} \nu \left( \frac{2\pi nk}{\omega_c} + \frac{d_0}{c} \right). \quad (6)$$

The 1s in (4), (5), and (6) represent the carrier component of the received signal and are removed by the wall filter in a Doppler instrument. The remaining signal describes the target's oscillation. This result is consistent with the results of Holen *et al.* [9] when small amplitudes were applied to their equation. When the FFT of  $r_d(t)$  is displayed as a Doppler spectrum, the result will be horizontal bands in the Doppler spectral display at  $\pm\omega_0$  Hz.

This derivation did not consider the angle of incidence of the ultrasound beam to the target. The beam angle may be accounted for by scaling the vibration amplitude  $A$  by a factor of  $\cos \theta$ . Varying the angle between the ultrasound beam and the plane of target vibration does not alter the frequency of the target vibration and, therefore, does not alter the frequency content of the demodulated Doppler signal. The only effect of varying  $\theta$  is to diminish the amplitude of the Doppler signal.

#### E. Simulation of Flow Signals

The flow profile of a fluid in a tube depends on the viscosity of the fluid and the rate of flow, as well as the presence of any disturbances to flow within the tube. For low flow rates (i.e., those with a Reynolds number below 2000), a sufficient distance from any disturbance to flow, a parabolic flow profile develops. The velocity profile flattens from a true parabola with increasing flow rate, becoming uniform in the limit of high velocity. A parabolic flow profile produces a uniform Doppler spectral display; flatter profiles result in a greater emphasis of high frequencies when the vessel is uniformly insonified [1]. In the limit of a uniform flow profile, the Doppler signal is a delta function in the frequency domain, neglecting beam modulation effects.

To produce a display similar to that observed with a parabolic flow profile with a vibrating target, a signal with a uniform spectrum up to some cut-off frequency is required. A bandlimited noise source can be constructed to satisfy this requirement. Here, a summation of random-phase cosines was used to generate the bandlimited noise. The signal is given by

$$s(t) = \sum_{n=0}^N \cos(\omega_0 n t + \phi_n)$$

where each  $\phi_n$  represents a random variable uniformly distributed on  $(-\pi, \pi)$ . The Fourier transform of this signal is a collection of delta functions of equal strength  $\omega_0$  radians apart from  $-N\omega_0$  to  $N\omega_0$ . The value of  $\omega_0$  is chosen to be sufficiently small so that the individual deltas are not resolved by the FFT used to generate the Doppler spectral displays. For the signals used in the experiments,  $\omega_0$  was chosen to be  $2\pi/4096$ , rendering the individual deltas quite invisible to the 128- or 256-point FFTs used to examine the Doppler signals.

When  $s(t)$  is used to drive the target, the resulting Doppler spectral display is uniform from  $-N\omega_0/2\pi$  to  $N\omega_0/2\pi$  Hz as long as the restrictions on vibration amplitude are observed. Although the signal here was chosen to have a flat spectrum, by appropriate weighting of the cosines, any desired spectral distribution may be developed to simulate non-parabolic flow profiles.

The velocity of flow in the arteries varies with time and is associated with the cyclic pulsation characteristic of the human circulatory system. It would be desirable to model this with the vibrating thin film target. This may be achieved by varying the bandwidth of the vibration signal described previously with time. To simulate periods of slow flow, the bandwidth is reduced; increasing the noise bandwidth simulates higher velocities.

To construct this signal, the following technique may be used. Let  $\nu_p(t)$  be a signal that describes the peak simulated Doppler frequency shift versus time. For normal arterial flow,  $\nu_p(t)$  is expected to be quasi-periodic on the scale of a second or so. Fig. 2 shows the  $\nu_p(t)$  used in these

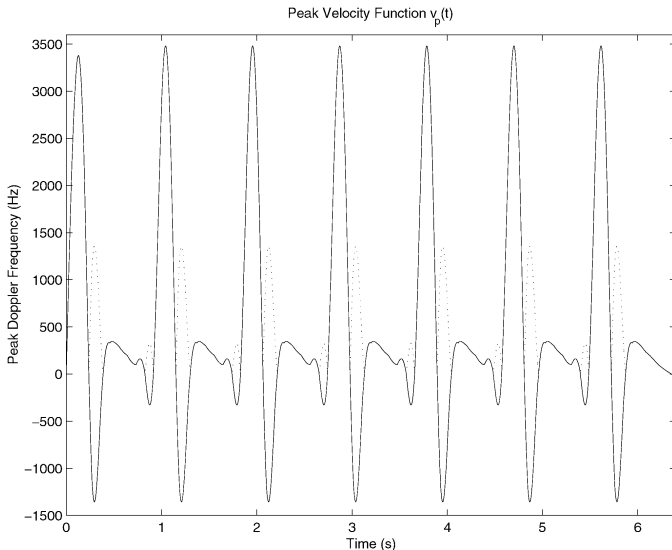


Fig. 2. Peak velocity function used in the generation of the synthetic arterial drive signal.

experiments. We constructed the drive signal  $s(t)$  according to the equation

$$s(t) = \sum_{n=0}^{\infty} m_n(t) \cos(\omega_0 n t + \phi_n)$$

where

$$m_n(t) = \begin{cases} 1 & \text{if } \nu_p(t) \geq n\omega_0 \\ 0 & \text{if } \nu_p(t) < n\omega_0; \end{cases}$$

$m_n(t)$  is a windowing function used in combination with  $\nu_p(t)$  to determine which random-phase sinusoids to include in the summation at a given instant.  $m_n(t)$  passes all the sinusoids of frequency up to and including the value of  $\nu_p(t)$  to the summation. Thus, at time  $t$ ,  $s$  is the summation of random phase sinusoids of frequencies up to and including those less than the value of  $\nu$  at time  $t$ .

The bandwidth of  $s(t)$  does not strictly follow  $\nu(t)$ , because the switching of cosines in and out of the summation introduces high frequency components. In effect, the cosines are multiplied with square-wave functions. The result in the frequency domain is the convolution of the transform of the square wave with the desired spectrum.

### III. EXPERIMENT

The mechanical details of the experimental setup are illustrated in Fig. 3. The film is made of Vesicular (Xidex Corporation) microfiche film. The scatterers in the film exist as collections of small ( $\sim 1 \mu\text{m}$ ) nitrogen gas bubbles within the film, generated through a photographic exposure and development process. The bubbles are patterned in halftone fashion to generate the desired target shape [12]. The film is held flat and in tension by a set of four springs attached at the ends of the support rails and the walls of the tank. The tank is filled with degassed,

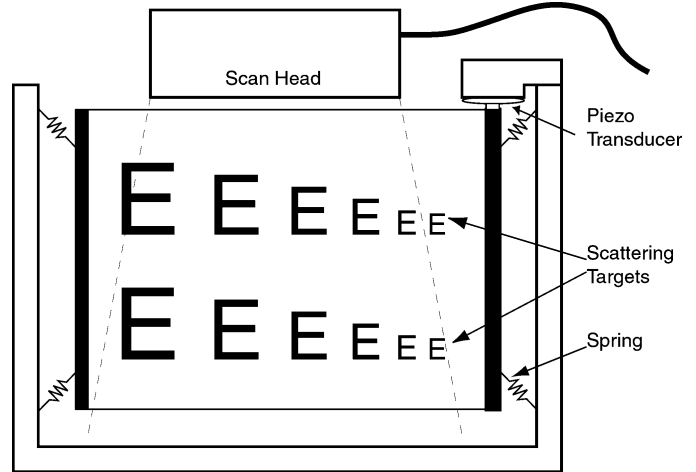


Fig. 3. Schematic drawing of the mechanical setup used in the experiments. The thin film target is located within the scan plane of the transducer. The target motion is in the plane of the page, toward and away from the transducer.

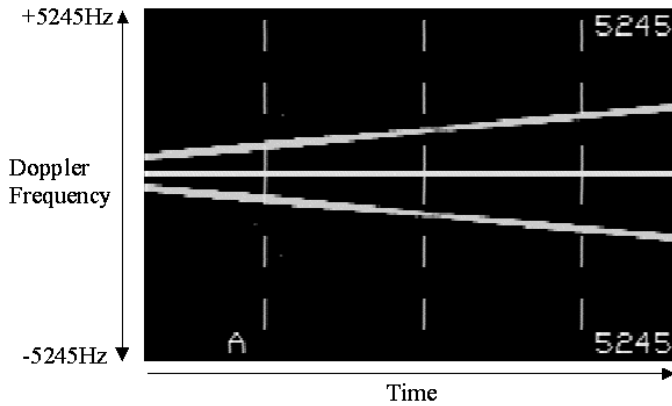
de-ionized water in these experiments, to eliminate effects caused by attenuation. The phantom is normally designed for use with an acoustically non-scattering, attenuating medium. A piezoelectric disk transducer, which drives the thin film target, is attached to the upper end of one rail. When a voltage excitation is applied to the transducer, the rail and film are driven into motion in a vertical plane, relative to the illustrated setup.

A small circuit was constructed to convert digital waveforms, synthesized in MATLAB according to the equations given in Section II, into an analog drive signal for the piezoelectric element of sufficient amplitude to achieve the desired effect. Four drive signals were generated: the arterial signal, linear and logarithmic frequency sweeps, and a melodious sequence of pure tones. The synthesized waveform vectors were stored in an EPROM. The circuit converts the waveform samples to an analog voltage at a 10-kHz sampling rate. The overall signal gain is adjustable to provide a maximum output of 80 V peak-peak. The signal source was constructed as a matter of convenience; any source with sufficient drive capacity would do.

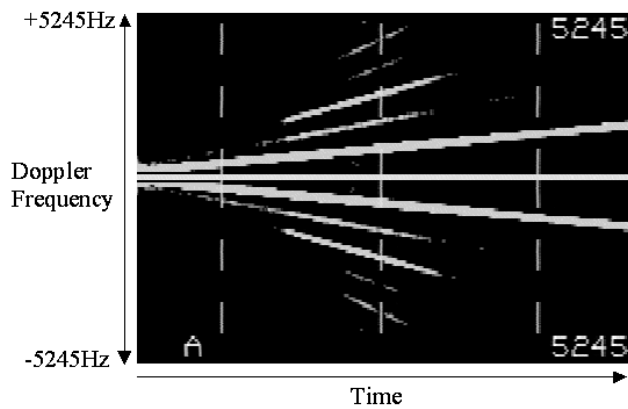
The film was scanned in these experiments with a Quantum QAD-1 scanner (Siemens Medical Systems, Inc., Ultrasound Group, Issaquah, WA) operated in PW Doppler mode. A 7.5-MHz transducer was used, fixed in a clamp over the film in a manner such that the thin film target was in scan plane.

### IV. RESULTS

Figs. 4 and 5 are Doppler spectral displays captured from the QAD-1 scanner. The Doppler spectral display in Fig. 4(a) was generated with a low amplitude frequency sweep. The drive signal varies linearly from 0 to 3 kHz in 6.4 s. Because this amounts to a frequency shift of only 6 Hz within a Doppler FFT window, the drive frequency



(a)



(b)

Fig. 4. PW Doppler spectra captured with the Quantum QAD-1 ultrasound system for a) low amplitude and b) high amplitude vibration.

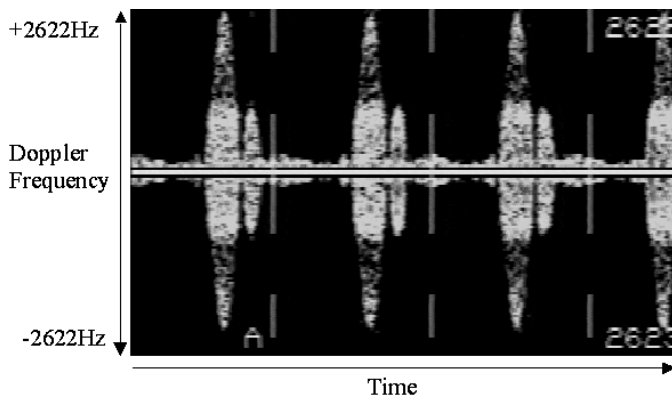


Fig. 5. PW Doppler spectrum observed with the simulated arterial signal.

is essentially constant within any given FFT. As a result, there are only signal components at the base drive frequency  $\omega(t)$ , as predicted by the theory. In Fig. 4(b), the Bessel band phenomenon discussed in [9] is illustrated, where the same frequency sweep signal, as in Fig. 4(a), is used, but the amplitude has been increased by a factor of  $\sim 5$ . The Doppler signal is clearly visible at multiples of the vibration frequency  $\omega$ .

A synthesized arterial signal is shown in Fig. 5. The distribution of velocities up to the maximum velocity is visible. The peak velocity function  $\nu(t)$  is also shown. Because of the symmetrical nature of the sonographs generated with this technique, the reverse flow section of  $\nu(t)$  appears as a smaller hump in the sonograph.

## V. DISCUSSION

The described system provides significant potential for evaluating CW and PW Doppler systems. The vibrating target produces a well-controlled stimulus to a Doppler system. The response of the system to the known signal can be used to assess system performance in terms of Doppler sensitivity and uniformity of spectral response. Work by Jensen [13] has shown that wall filters used in Doppler systems have a significant impact on the SNR of the Doppler signal and the stability of the resulting velocity estimate.

The vibrating target does produce a signal that can be detected by Kasai-type Color Flow Doppler (CFD) systems [14]. However, the Kasai algorithm estimates the mean flow velocity within a resolution cell. Because the Doppler signal produced is bi-directional, estimates of the mean velocity will tend toward zero. Thus, the vibrating thin film target does not provide a suitable stimulus for the evaluation of the mean velocity estimation accuracy of the CFD system. Signals may be synthesized that allow one-sided spectra to be generated (low frequency sawtooth waves), but they tend to be difficult to realize with a simple mechanical system. The vibration of the target and the activation of the CFD do allow an evaluation of CFD spatial resolution as demonstrated in earlier work by Phillips [10]. For correlation-type Doppler processors [11], [15], it would be necessary to synchronize the motion of the thin film with the Doppler acquisition and processing in order to satisfy the underlying assumptions of correlation systems and obtain meaningful Doppler data.

## VI. CONCLUSION

We have presented a means for simulating a Doppler detectable flow velocity distribution using a single vibrating thin film target. By vibrating a target with a bandlimited noise signal, an echo signal is produced that is interpreted by CW and PW Doppler as a distribution of velocities, the weighting of any given velocity determined by the characteristics of the noise signal spectrum. We have also demonstrated the ability to simulate a time-dependant flow velocity distribution by varying the signal bandwidth with

time. Thus, it is possible, by combining the velocity weighting and time-varying velocity techniques, to create a signal that resembles a realistic replica of arterial flow normally displayed by a CW or PW Doppler spectral display.

#### ACKNOWLEDGMENTS

The authors are grateful for collaboration with Robert Naum of Applied Image, Inc. and the constructive comments of the anonymous reviewers.

#### REFERENCES

- [1] J. A. Jensen, *Estimation of Blood Velocities Using Ultrasound: A Signal Processing Approach*. Cambridge, England: Cambridge University Press, 1996.
- [2] P. R. Hoskins, T. Anderson, and W. N. McDicken, "A computer controlled flow phantom for generation of physiological Doppler waveforms," *Phys. Med. Biol.*, vol. 14, no. 11, pp. 1709–1717, Nov. 1989.
- [3] W. N. McDicken, "A versatile test-object for the calibration of ultrasonic Doppler flow instruments," *Ultrason. Med. Biol.*, vol. 12, no. 3, pp. 245–249, Mar. 1986.
- [4] D. W. Rickey, P. A. Picot, D. A. Christopher, and A. Fenster, "A wall-less vessel phantom for Doppler ultrasound studies," *Ultrason. Med. Biol.*, vol. 21, no. 9, pp. 1163–1176, Sep. 1995.
- [5] E. J. Boote and J. A. Zagzebski, "Performance tests of Doppler ultrasound equipment with a tissue and blood-mimicking phantom," *J. Ultrason. Med.*, vol. 7, no. 3, pp. 137–147, Mar. 1988.
- [6] S. V. Russell, D. McHugh, and B. R. Moreman, "Programmable motion Doppler string test object," *Phys. Med. Biol.*, vol. 38, no. 11, pp. 1623–1630, 1993.
- [7] D. W. Rickey and A. Fenster, "A Doppler ultrasound clutter phantom," *Ultrason. Med. Biol.*, vol. 22, no. 6, pp. 747–766, 1996.
- [8] W. N. McDicken, D. C. Morrison, and D.S.A. Smith, "A moving tissue-equivalent phantom for ultrasonic real-time scanning and Doppler techniques," *Ultrason. Med. Biol.*, vol. 9, no. 4, pp. L455–L459, Jul.-Aug. 1983.
- [9] J. Holen, R. C. Waag, and R. Gramiak, "Representations of rapidly oscillating structures on the Doppler display," *Ultrason. Med. Biol.*, vol. 11, no. 2, pp. 267–272, Mar.-Apr. 1985.
- [10] D. Phillips, S. McAleavey, and K. J. Parker, "A new thin film phantom for performance evaluation of ultrasonic Doppler imaging systems," in *1996 IEEE Ultrason. Symp. Proc.*, vol. 2, pp. 1201–1204.
- [11] O. Bonnefous and P. Pesque, "Time domain formulation of pulse-Doppler ultrasound and blood velocity estimation by cross correlation," *Ultrason. Imaging*, vol. 8, no. 2, pp. 73–85, Apr. 1986.
- [12] S. A. McAleavey, R. G. Naum, and K. J. Parker, "Characterization of a thin film phantom for contrast and resolution measurements," in *Proc. SPIE—The Int. Soc. Opt. Eng.*, vol. 3658, 1999, pp. 530–537.
- [13] J. A. Jensen, "Stationary echo canceling in velocity estimation by time-domain cross-correlation," *IEEE Trans. Med. Imaging*, vol. 12, no. 3, pp. 471–477, Sep. 1993.
- [14] C. Kasai, K. Namekawa, A. Koyano, and R. Omoto, "Real-time two-dimensional blood flow imaging using an autocorrelation technique," *IEEE Trans. Sonics Ultrason.*, vol. SU-32, no. 3, pp. 458–464, May 1985.
- [15] I. A. Hein, J. T. Chen, W. K. Jenkins, and W. D. O'Brien, Jr., "A real-time ultrasound time-domain correlation blood flowmeter. I. Theory and design," *IEEE Trans. Ultrason., Ferroelect., Freq. Contr.*, vol. 40, no. 6, pp. 768–775, Nov. 1993.



**Stephen McAleavey** was born in Danbury, Connecticut in 1974. He received the B.S. and M.S. degrees in electrical engineering in 1996 and 1998, respectively, both from the University of Rochester, Rochester, NY. He is presently pursuing the Ph.D. in electrical and computer engineering at the University of Rochester. Since 1996, he has held positions as Teaching and Research Assistant at the University of Rochester. His teaching responsibilities have included lectures on medical imaging and Doppler ultrasound. His research interests are in the area of ultrasound imaging, Doppler techniques, and implementation signal processing techniques. He is a member of IEEE and Tau Beta Pi.



**Zaegyoo Hah** was born in Taejeon, Korea in 1962. He received B.S., M.S., and Ph.D. degrees in electronic engineering in 1985, 1988, and 1993, respectively, from Seoul National University, Seoul, Korea. He is Associate Professor of Electronic Engineering at KongJu National University, KongJu, Korea. His research interests include ultrasonic propagation, underwater beamforming, and medical applications of ultrasound. He is currently a visiting scientist at the University of Rochester, Rochester, NY, working with

Kevin Parker in the area of thin film phantoms and tissue-mimicking materials.



**Kevin J. Parker** (S'79–M'81–SM'87–F'95) received the B.S. degree in engineering science, *summa cum laude*, from SUNY at Buffalo in 1976. Graduate work in electrical engineering was done at MIT, with M.S. and Ph.D. degrees received in 1978 and 1981 for work in electrical engineering with a concentration in bioengineering. Dr. Parker is Professor of Electrical and Computer Engineering, Radiology, and Bioengineering at the University of Rochester, where he has held positions since 1981. In 1998, Dr. Parker was named Dean of the School of Engineering and Applied Sciences at the University of Rochester. Dr. Parker has received awards from the National Institute of General Medical Sciences (1979), the Lilly Teaching Endowment (1982), the IBM Supercomputing Competition (1989), the World Federation of Ultrasound in Medicine and Biology (1991), and the Joseph P. Holmes Pioneer Award from the AIUM (1999). He is a member of the IEEE, the Acoustical Society of America, and the American Institute of Ultrasound in Medicine. He was named a Fellow in both the IEEE and the AIUM for his work in medical imaging and in the ASA for his work in acoustics. In addition, he recently completed a three-year term on the Board of Governors of the AIUM. Dr. Parker's research interests are medical imaging, linear and nonlinear acoustics, and digital halftoning.